

Chemiluminescence Studies of the Reaction between O(³P) Atoms and Methyl IodideBess C. L. Kwong[†] and R. S. Tse^{*}

Department of Chemistry, University of Hong Kong, Pokfulam Road, Hong Kong

Received: July 11, 1993; In Final Form: November 1, 1993[⊙]

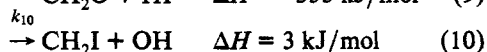
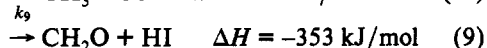
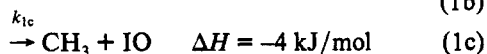
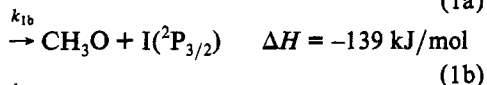
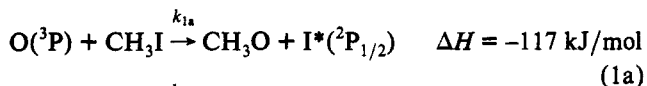
The reaction between O(³P) atoms and CH₃I was studied in a fast discharge–flow system. A threshold behavior with respect to the ratio of initial reactant concentrations in the chemiluminescence due to I₂ (B²Π_{0_g⁺} → X¹Σ_g⁺) was observed. The reactions in Chart 1 were considered significant in our interpretation. Fitting of temporal profiles produced an order of magnitude for *k*₁ of 10¹⁰ cm³ mol⁻¹ s⁻¹ at room temperature. Chemiluminescence from OH(A²Σ → X²Π)_(0,0), OH(X)_(2→1,1→0), CO(X)_(1→0), and CO₂(X)_(ν₃=1→0) was also observed, in common with observations of O(³P) reactions with hydrocarbons.

Introduction

Methyl iodide is a molecule of intense interest to reaction dynamicists and kineticists. Its photochemistry has been extensively studied. Its reactions with some atoms and with ozone have been studied. Its reaction with oxygen atoms, a reaction of importance in combustion and atmospheric chemistry, is, however, almost unknown.

As early as 1969, Herron and Huie¹ attempted to study the reaction between O(³P) atoms and methyl iodide. They encountered massive deposits on reactor walls and found formaldehyde and oxides of iodine among the deposits. They nevertheless deduced that O(³P) reacted with methyl iodide at a much faster rate than with other monohaloalkanes, which reacted through hydrogen abstraction.

Recently Grice *et al.*² reported a crossed molecular beam study of O(³P) reactions with a few alkyl iodides, which did not include methyl iodide. The reaction between O(³P) and methyl iodide is expected to have the following possible channels:

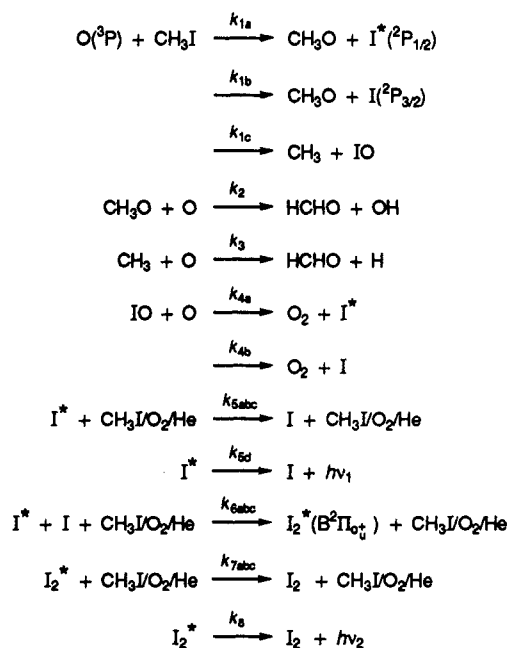


We have studied the reaction between O(³P) atoms and CH₃I by monitoring mainly the chemiluminescence produced in iodine atom recombination.

Experimental Details

We studied the reaction in a conventional discharge–flow system at ~1 Torr of pressure and at a linear flow rate of ~1 cm/ms, pumped by Roots pumps. Two different reactors were used, both of 25-mm internal diameter. The end-on reactor, shown in Figure 1, with argon blowing at the inside of the observation window to reduce deposits, was used to characterize the products. A more conventional side-on reactor, shown in Figure 2, was used to quickly monitor the temporal profile of the products. Quartz

CHART 1



windows were used in the UV–vis range and CaF₂ windows in the infrared. Normally the inside wall of the reactor was not coated, but we found that a coating of syrupy phosphoric acid would enhance OH(X)_(2→1,1→0) signals.

Two methods of generating O(³P) were used, both in a carrier of He. One was the well-known N + NO titration, and the initial [O(³P)] was obtained from the NO flow rate. The other was the direct microwave discharge of O₂ in He, and the initial [O(³P)] was obtained from NO₂ titration. In our system, the former method produced only ~0.05 Torr of O(³P). The latter method produced higher initial [O(³P)] and allowed easier characterization of the reaction. Such a discharge is known to produce O₂(¹Δ_g), but not much of it can be expected under our experimental conditions.³ We also experimented with killing O(³P) in such a discharge stream with a Hg film on the reactor wall downstream from the discharge. No reaction was observable. This showed that O₂(¹Δ_g) did not initiate a reaction under the experimental conditions.

Characterization of the chemiluminescence in the UV–vis range was made through a monochromator (which had been salvaged from a discarded Varian Techtron 1200 atomic absorption spectrometer and had a resolution of ~1 Å), but the temporal profile of the chemiluminescence was recorded through suitable filters. Intensities were measured with a Hamamatsu R446 photomultiplier, whose signal was fed through an SRS SR-240

[†] Present address: Centre for Molecular Beams and Laser Chemistry, Department of Chemistry, University of Waterloo, Waterloo, Ontario N2L 3G1, Canada.

^{*} Author to whom correspondence should be addressed. E-mail address: hrscism@hkucc.hku.hk.

[⊙] Abstract published in *Advance ACS Abstracts*, January 1, 1994.

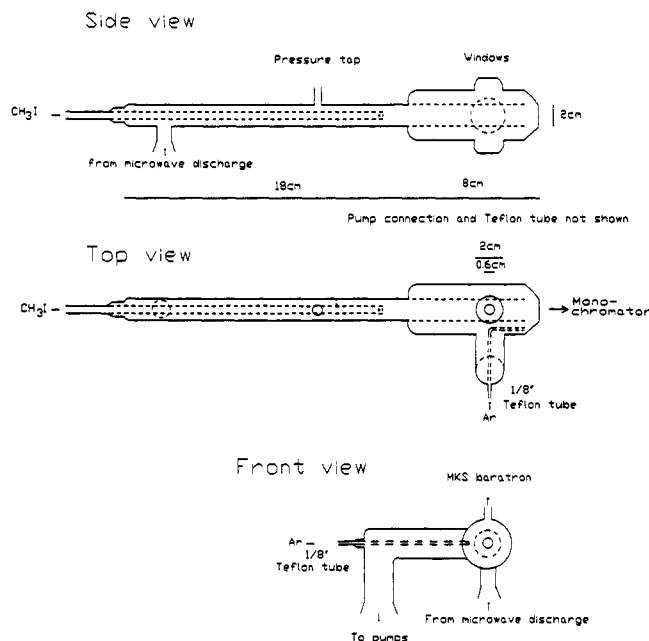


Figure 1. End-on reactor.

preamplifier usually to a digital voltmeter. Chemiluminescence in the infrared was studied with a Nicolet 170SX FT spectrometer.

Second-order intensities produced by the monochromator were checked with the aid of a mercury lamp and a filter which passed 90% in the range 300–400 nm but cut off very sharply at both ends of the transmitting range. Second-order intensities were found to depend on slit width and to be considerable.

At one stage we tried to observe the laser-induced fluorescence (LIF) of IO. We used a PRA LN1000 nitrogen laser to pump an LN102 dye laser and a frequency doubler.

He, Ar, O₂, and N₂ were supplied by Hong Kong Oxygen. The claimed purities were >99.99%, >99.99%, >99.5%, and >99.995%, respectively. The moisture impurity in each was absorbed by molecular sieve traps.

NO with a claimed purity of >99.0% was supplied by Matheson. A mass spectrometric analysis showed actual purity of 97.7%, with impurities of air and NO₂.

NO₂ for titration purpose was generated from the reaction of copper turnings with concentrated nitric acid. After purification by bulb-to-bulb distillation, the purity was determined by mass spectrometric analysis to be 91%, with the impurities consisting of air, NO, and N₂O.

Methyl iodide supplied by Merck had a claimed purity of >99%. It was bulb-to-bulb distilled and stored in the dark at most 1 week before use.

All the above gases were made to go through suitable cold traps before they were allowed to enter the reactor.

Results

Chemiluminescence in the UV–vis Range. The prominent feature of chemiluminescence in the UV–vis range from the O(³P) + CH₃I reaction lies in the 500–700-nm range, as shown in Figure 3. The broad feature is characteristic of the I₂ B²Π_{0_g⁺} → X¹Σ_g⁺ emission⁴ from I atom recombination, designated as I₂* below.

Other than the above, the well-known OH(A²Σ → X²Π)_(0,0) emission at 309 nm was very strong. The sharp feature in Figure 3 was the monochromator second-order effect of the OH(A–X) emission.

To avoid the problem of deposits on windows, spectral data such as those shown in Figure 3 were painstakingly and manually acquired. To measure spectral intensities over a small wavelength range, the background signal without CH₃I flow was taken at the

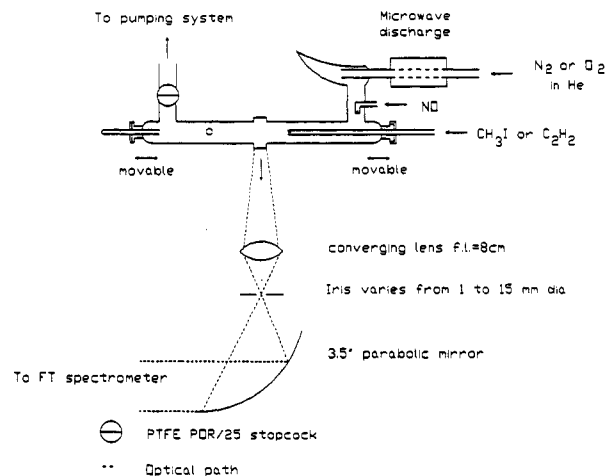


Figure 2. Side-on reactor.

beginning of the range. The intensity with CH₃I flow was then taken and the monochromator moved to another wavelength, usually 1 nm away. The same two intensity readings were taken. After a number of wavelength settings the monochromator was returned to the first wavelength of the range, and the intensity readings were taken again. If the first intensities agreed with the last readings, the values in between were considered to be valid. If they did not agree, indicating some deposits had accumulated on the window, the set of data was discarded. What are shown in Figure 3 constitute valid net intensity readings.

A filter (OY2) transmitting in the range 500–700 nm and the photomultiplier were used to monitor the variations of I₂* intensities with other variables.

Variations of I₂* intensity in the range 500–700 nm with initial reactant flow rates are shown in Figure 4. It appears that there is a threshold for the appearance of emission, and this threshold is dependent on both initial O(³P) atom flow rate and initial CH₃I flow rate. These threshold conditions are listed in Table 1.

The temporal profile of the emission in the range 500–700 nm could be obtained with the side-on reactor only within a small range of reactant flow rates. The measured values limited by error bars and the calculated line are shown in Figure 5.

Chemiluminescence in the Infrared. OH(X)_(2→1,1→0), CO(X)_(1→0), and CO₂(X)_(ν₃=1→0) emissions were observed.

Infrared Absorption of Deposit. We managed to obtain infrared absorption spectra of deposits on windows both before and after exposure to moist air. The spectra show the presence of formaldehyde and polyiodates, in agreement with the observation of Herron and Huie.¹ Since the deposits ought to have been products of reactions downstream to the reaction in question, little effort was spent in further characterizing them.

Discussion

Of the probable reaction channels (1a), (1b), (1c), (9), and (10) listed above, reaction channel (9) is highly exoergic, but we have not been able to observe any signal of HI in emission or in absorption. For reaction (9) to be significant, a complex has to be formed; subsequent rearrangement will be necessary to eliminate HI from the complex. The reaction of F atoms with CH₃I produces no HI,^{5–7} but then F atoms are more electronegative than O atoms. Nevertheless, reaction (9) is probably insignificant.

Reaction (10) is essentially thermal neutral and is a hydrogen abstraction reaction analogous to O(³P) reactions with mono-haloalkanes whose rate constants are ~2–3 orders of magnitude lower than reaction (1).¹ The reaction between F atoms and CH₃I, however, does produce HF.^{6,7} The reaction is fast and is exoergic to 153 kJ/mol. The heat of formation of F atoms is 79

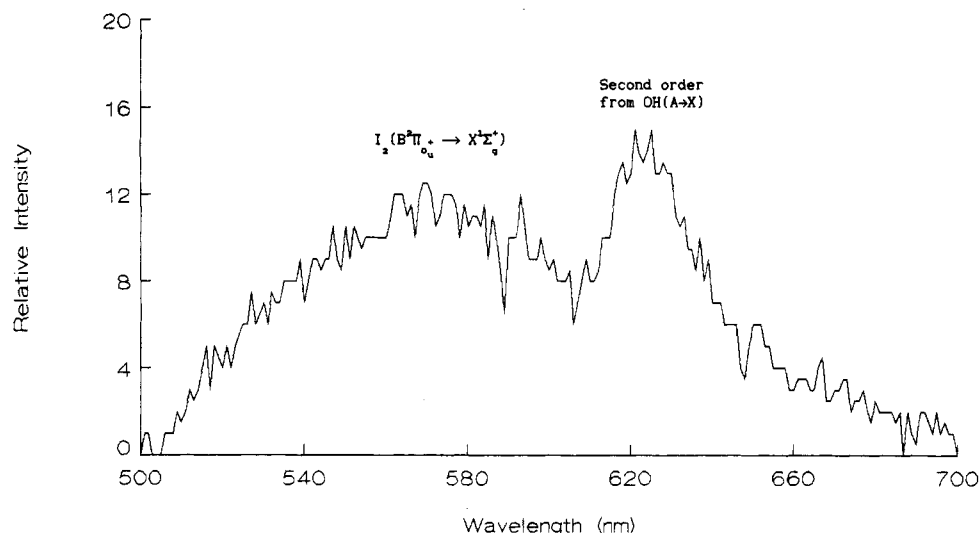


Figure 3. Chemiluminescence from the reaction of O(³P) with CH₃I in the spectral range 500–700 nm. The end-on reaction chamber was used.

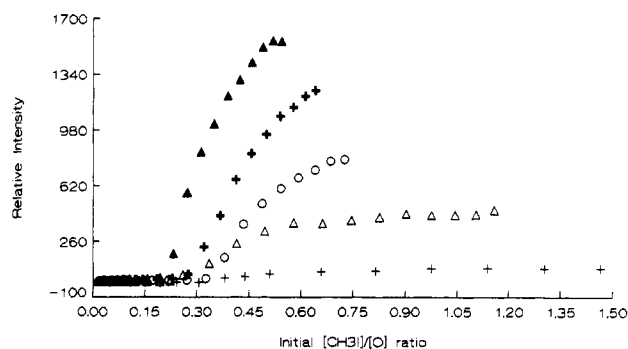


Figure 4. Variations of detected intensity of I₂* with different initial [CH₃I]/[O] ratios. The end-on reactor was used. Signals were collected through the OY2 band filter. O(³P) pressures in Torr: +, 0.075; Δ, 0.141; ○, 0.203; +, 0.243; ▲, 0.268.

TABLE 1: Conditions at Thresholds in Figure 4

experimental ^a				calculated ^b			
[O(³ P)] ₀	[CH ₃ I] ₀	[O] ₀ /[CH ₃ I] ₀	[O ₂] ₀	A	B	C	I
0.075	0.0285	2.6	0.048	1.43	0.29	2.51	99
0.141	0.0317	4.5	0.111	1.50	0.64	8.99	210
0.203	0.0298	6.8	0.226	1.60	1.27	18.5	206
0.243	0.0337	7.2	0.378	1.79	2.11	26.6	255
0.268	0.0319	8.4	0.481	1.90	2.68	32.3	233

^a Partial pressures in Torr. ^b In self-consistent units. *I* is the calculated intensity at the threshold. For definitions of *A*, *B*, and *C*, please see text under Discussion.

kJ/mol, but that of O atoms is 249 kJ/mol. Thus reaction (10) is not expected to be important in the reaction between O atoms and CH₃I.

However, a Walden inversion in the gas phase has been observed for the F-atom analogue (F + CH₃I → FCH₃ + I)⁸ of reactions (1a) and (1b). The rate constants for thermal atom substitution reactions F + CH₃X (where X = Cl, Br, I) → FCH₃ + X increase as the exothermicity of the replacement reaction increases and as the CH₃-X bond dissociation energy decreases.⁹ This is similar to the O + CH₃X analogue in previous¹ and present studies.

Reaction (1c) is expected to produce ground-state IO. We have attempted to observe it with laser-induced fluorescence (LIF), but to no avail. The detectability of our LIF system was about 10⁹–10¹⁰ species/cm³. Grice *et al.*² used a mass spectrometer detector to monitor the IO product in crossed molecular beam experiments of O atom reactions with alkyl iodides. The smallest alkyl group they selected was the ethyl group. Their experiments did not favor⁸ the possibility of Walden inversion to produce I

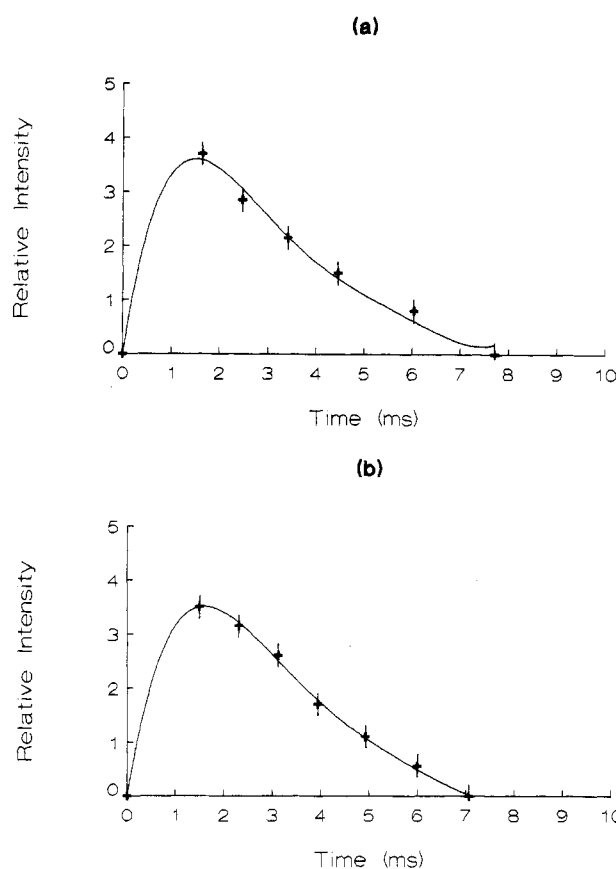


Figure 5. Decay profile of I₂* in the spectral range 500–700 nm. The side-on reactor was used. Linear flow rate was ~1 ms/cm. Initial partial pressures in Torr. (a) CH₃I, 0.39; O(³P), 0.04; O₂, 0.04; He, 0.96. (b) CH₃I, 0.19; O(³P), 0.05; O₂, 0.04; He, 1.11. Experimental points are marked by error bars. Calculated values are linked by solid lines for display purposes only.

atoms but encouraged an R–I–O transition complex that would decompose into R and IO, similar to reaction channel (1c) here.

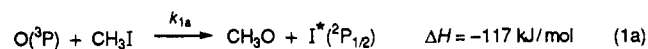
Lee *et al.*¹² and Gorry *et al.*¹³ found IO in crossed molecular beam studies of O + CF₃I. But Worsdorfer *et al.*⁵ and Venkitachalam *et al.*⁸ have shown that



can only be a minor channel for the production of IO in that system, and IO must be mainly produced through direct reaction analogous to reaction channel (1c) here.

CHART 2

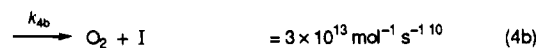
I* and I production



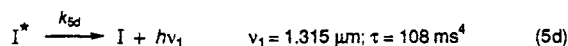
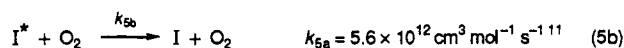
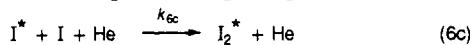
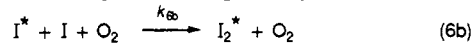
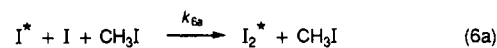
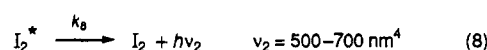
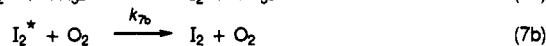
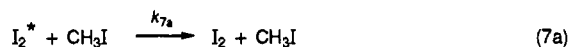
reaction of primary products with O(^3P)



$$k_2 = 6 \times 10^{12} \text{ cm}^3 \text{ mol}^{-1} \text{ s}^{-10}$$



I* quenching and emission

I* and I recombination to form I₂*⁴I₂* quenching and emission

Our inability to observe IO may be due to our instrumental limitations. More likely, though, is the possibility that the steady-state concentration of IO even under low [O] conditions is too low to be observed. One interesting observation is that those who have observed IO^{2,12,13,16} have not reported any deposits.

I₂* Formation and Emission. The source of I₂* is most probably the recombination of I* and I through the reactions shown in Chart 2.

Simulation of I₂* Temporal Profile. From reactions (1)–(8), rate expressions can be developed for d[O]/dt, d[CH₃O]/dt, d[CH₃]/dt, d[IO]/dt, d[I*]/dt, d[I]/dt, d[I₂*]/dt, and d[hν₂]/dt.

We neglect a number of possible reactions. CH₃ + OH → CH₃OH was considered unimportant because one reactant is a tertiary product and both reactants would be very low in concentration. CH₃I + I → CH₃ + I₂ was neglected because it has a low rate constant (6.6 × 10⁻¹ cm³ mol⁻¹ s⁻¹ at 300 K¹⁰) and because a large isotope effect has been observed for the quenching of I* by CH₃I and CD₃I.¹⁴ HCHO + O → OH + HCO was neglected for the same reason and because HCHO was a tertiary product and [O] was low under our experimental conditions for temporal profile measurements. We have neglected the reaction O + I₂ → OI + I (k = 8 × 10¹³ cm³ mol⁻¹ s⁻¹⁰) because [O] was low, I₂ was a tertiary product, and IO was not observed. We

TABLE 2: Coefficients for the Simulation of the Temporal Profile of Intensity

coefficient	Figure 5a	Figure 5b
BO	0.02606	0.1133
GO	15.272	17.066
k ₁ '[CH ₃ I] ₀ (s ⁻¹)	0.479	0.419
EO	-0.183	-0.755
n (data sets)	7	8
(ΣΔ ² /n) ^{1/2}	0.13	0.06
k ₁ ' (cm ³ mol ⁻¹ s ⁻¹)	2.4 × 10 ¹⁰	4.5 × 10 ¹⁰

have also neglected energy-transfer reactions involving O₂(¹Δ_g), which should have a very low concentration under our experimental conditions.³

We can assume steady-state conditions for [CH₃O], [CH₃], and [IO]. After simple algebraic manipulations, the following can be obtained:

$$\begin{aligned} d[\text{O}]/dt = & -k_1[\text{CH}_3\text{I}][\text{O}] - (k_{1a} + k_{1b})[\text{CH}_3\text{I}][\text{O}] - \\ & k_{1c}[\text{CH}_3\text{I}][\text{O}] - k_{1c}[\text{CH}_3\text{I}][\text{O}] \\ & \text{where } k_1 = k_{1a} + k_{1b} + k_{1c} \end{aligned}$$

$$= -(2k_1 + k_{1c})[\text{CH}_3\text{I}][\text{O}]$$

$$= -(2k_1 + k_{1c})[\text{CH}_3\text{I}]_0[\text{O}]$$

when [CH₃I]₀ ≫ [O]₀ as in Figure 5, where the subscript indicates reaction time

$$= -k_1'[\text{CH}_3\text{I}]_0[\text{O}] \quad \text{where } k_1' = 2k_1 + k_{1c}$$

Integration gives [O]_t = [O]₀ exp(-k₁'[CH₃I]₀t).

[I*]_t and [I]_t can then be expressed in terms of [CH₃I]₀[O]_t, and [I₂*]_t can be deduced:

$$\begin{aligned} [\text{I}_2^*] = & \frac{k_6}{k_7 k_5 k_1'} (k_{1b} + k_{1a} + k_{1c} k_{4b}/k_4) (k_{1a} + k_{1c} k_{4a}/k_4) \times \\ & [\text{CH}_3\text{I}]_0 [\text{O}]_0^2 \{ \exp(-k_1'[\text{CH}_3\text{I}]_0 t) - \exp(-2k_1'[\text{CH}_3\text{I}]_0 t) \} \end{aligned}$$

where

$$k_4 = k_{4a} + k_{4b}$$

$$k_5 = k_{5a}[\text{CH}_3\text{I}] + k_{5b}[\text{O}_2] + k_{5c}[\text{He}] + k_{5d}$$

$$k_6 = k_{6a}[\text{CH}_3\text{I}] + k_{6b}[\text{O}_2] + k_{6c}[\text{He}]$$

$$k_7 = k_{7a}[\text{CH}_3\text{I}] + k_{7b}[\text{O}_2] + k_{7c}[\text{He}]$$

This expression takes the form

$$y = \text{BO} + \text{GO} \exp(-k_1' t + \text{EO}) - \text{GO} \exp(-2k_1' t + \text{EO})$$

Experimental conditions that produced Figure 5 were used to fit the above expression. The good fit shows that reactions (1a), (1b), and (1c) are the major channels of the reaction between O(^3P) and CH₃I. Conditions for Figure 5a ([CH₃I]₀ = 0.39 Torr, [O]₀ = 0.04 Torr) produced k₁' = 2.4 × 10¹⁰ cm³ mol⁻¹ s⁻¹; those for Figure 5b ([CH₃I]₀ = 0.19 Torr, [O]₀ = 0.04 Torr) produced k₁' = 4.5 × 10¹⁰ cm³ mol⁻¹ s⁻¹. Since the resultant value of k₁ is smaller than the rate constants of reactions (2)–(5), the assumption of steady-state conditions for [CH₃], [CH₃O], and [IO] was valid. Detailed values of the coefficients are shown in Table 2.

Since

$$k_1' = 2k_1 + k_{1c} = 2k_{1a} + 2k_{1b} + 3k_{1c}$$

then

$$k_1 \approx \frac{1}{2}k_1' = (1-2) \times 10^{10} \text{ cm}^3 \text{ mol}^{-1} \text{ s}^{-1}$$

In view of the indirectness of measurement and the assumptions made, the value for k_1 should be treated as an order of magnitude value and probably its lower limit.

The rate constant at 283 K of an analogous F atom equivalent of reactions (1a) and (1b) (i.e., $\text{F} + \text{CH}_3\text{I} \rightarrow \text{CH}_3\text{F} + \text{I}$) has been reported⁹ to be $5 \times 10^{11} \text{ cm}^3 \text{ mol}^{-1} \text{ s}^{-1}$. The electronegativity values of the F atom and the O atom are very close, 3.98 and 3.44, respectively, in the Pauling scale.¹⁵ In comparison to the value of the above rate constant, our value for k_1 must be considered to be reasonable.

The value of k_{1c} can also be compared with the rate constant of the O(³P) + CF₃I reaction which produces CF₃ + IO exclusively^{12,13} through a long-lived CF₃-I-O complex. Its rate constant has been reported¹⁶ to be $(6.6 \pm 1.8) \times 10^{12} \text{ cm}^3 \text{ mol}^{-1} \text{ s}^{-1}$, which is 300–600 times higher than k_1 . Both reactions (1c) and O + CF₃I are nearly thermoneutral¹⁷ and belong to the type $\text{X} + \text{YZ} \rightarrow \text{XY} + \text{Z}$. Extra strength of the broken bond Y-Z will cause a shift of the potential energy of the molecule YZ as a function of the distance Y-Z when X is far away. This means that the greater the strength of the Y-Z bond, the steeper the curve will be and hence the higher the activation energy, since the reactant and product potential curves will now intersect at a higher energy level. The CH₃-I bond is 13 kJ/mol stronger than the CF₃-I bond.¹⁸ If this difference manifests itself entirely in the raised energy barrier, the O + CF₃I reaction is expected to be ~200 times faster than reaction (1c) at room temperature. Though we have not managed to measure the branching ratio of reaction (1), k_{1c} is expected to be small but of the same order of magnitude as the overall k_1 . Thus, a difference of a factor of 300–600 between the two rate constants is reasonable.

Other Aspects of the Overall Reaction. Figure 4 shows a threshold phenomenon, and the experimental conditions for the thresholds are listed in Table 1. These conditions indicate that the minimum value of [CH₃I]₀ to produce observable I₂* emission is dependent on [O]₀. A larger [O]₀ value will cause an increase of minimum [CH₃I]₀ required to produce observable I₂* chemiluminescence signal.

Below the threshold, [O]₀ ≫ [CH₃I]₀ and

$$d[\text{CH}_3\text{I}]/dt = -k_1[\text{CH}_3\text{I}][\text{O}]_0$$

Then

$$[\text{CH}_3\text{I}]_t = [\text{CH}_3\text{I}]_0 \exp(-k_1[\text{O}]_0 t)$$

We can neglect reactions of IO, CH₃O, and CH₃ with O atoms, as the latter were in large excess. We can then express $d[\text{I}^*]/dt$, $d[\text{I}]/dt$, $d[\text{I}_2^*]/dt$, $d[\text{I}_2]$, and $d[h\nu_2]/dt$ in terms of [CH₃I]_t and [O]₀. Then

$$\text{integrated intensity} = \frac{k_8 k_6 k_{1a} (k_{1a} + k_{1b})}{k_7 k_1 k_5} [\text{CH}_3\text{I}]_0^2 [0.5 + 0.5 \exp(-2k_1[\text{O}]_0 t) - \exp(-k_1[\text{O}]_0 t)]$$

That is

$$I = \frac{A}{B} [\text{CH}_3\text{I}]_0^2 C$$

Experimental values at the threshold and values for A, B, C, and I are shown in Table 1. For the calculation of parameter C,

k_1 was set at $0.3 \text{ Torr}^{-1} \text{ s}^{-1}$ and t was set to 10 ms. It can be seen that the calculated values of I are roughly constant, with the exception of the lowest [O]₀ point, where our assumption of [O]₀ ≫ [CH₃I]₀ is probably not valid enough. This constant value of I is just the lowest intensity measurable.

The rising portion of the lines in Figure 4 were obtained under the conditions of the previous Discussion section. The plateau region indicates the end of the steady-state condition.

Figure 4 also shows that under very lean conditions very little I₂* emission was observed. In fact, under such lean conditions, CH₃I behaves similar to a hydrocarbon fuel. OH(A→X), OH(X)_(2→1,1→0), CO(X)_(1→0), and CO₂(X)_(ν₃=1→0) are commonly observed in such systems and are probably produced from the reaction between the excess O(³P) and secondary and tertiary products.

When I₂* was observed, the emission at 1.315 μm from reaction (5d) was expected. We tried to observe it with the FT spectrometer but to no avail. This was understandable because it was already not easy to monitor the I₂* emission in the range 500–700 nm with a photomultiplier, and there was little hope of capturing the near-infrared emission with an InSb detector.

Conclusions

We have shown that reactions (1a), (1b), and (1c) are major channels for the reaction of O(³P) atoms with methyl iodide. The order of magnitude of the rate constant has been estimated to be $10^{10} \text{ cm}^3 \text{ mol}^{-1} \text{ s}^{-1}$. We have not observed IO but cannot exclude that reaction channel, which is probably not significant under our experimental conditions.

Acknowledgment. This work has been supported in part by grants from the Hong Kong Research Grants Council and from the Committee on Research and Conference Grants. B.C.L.K. thanks the University of Hong Kong for the award of a Postgraduate Studentship and the Swire Foundation for a scholarship both for the period 1989–92.

References and Notes

- Herron, J. T.; Huie, R. E. *J. Phys. Chem.* **1969**, *73*, 1326.
- White, R. W. P.; Smith, D. J.; Grice, R. *Chem. Phys. Lett.* **1992**, *193*, 269.
- Arnold, S. J.; Ogryzlo, E. A.; Witzke, H. J. *Chem. Phys.* **1964**, *40*, 1769.
- Stephan, K.-H.; Comes, F. J. *Chem. Phys. Lett.* **1979**, *65*, 251.
- Worsdorfer, U.; Heydtmann, H. *Ber. Bunsenges. Phys. Chem.* **1988**, *93*, 1132.
- Iyer, R. I.; Rowland, F. S. *J. Phys. Chem.* **1981**, *85*, 2493.
- Stein, L.; Wanner, J.; Walther, H. *J. Chem. Phys.* **1980**, *72*, 1128.
- Venkitachalam, T. V.; Das, P.; Bersohn, R. *J. Am. Chem. Soc.* **1983**, *105*, 7452.
- Iyer, R. S.; Rowland, F. S. *J. Phys. Chem.* **1981**, *85*, 2488.
- National Institute of Standards and Technology *Chemical Kinetics Data Base*, Ver. 4.0, Washington, D.C., 1992.
- Donovan, R. J.; Husain, D. *Chem. Rev.* **1970**, *70*, 508.
- Buss, R. J.; Sibener, S. J.; Lee, Y. T. *J. Phys. Chem.* **1983**, *87*, 4840.
- Gorry, P. A.; Nowikow, C. V.; Grice, R. *Mol. Phys.* **1979**, *38*, 1485.
- Fotakis, C.; Donovan, R. J. *J. Chem. Soc., Faraday Trans. II* **1978**, *74*, 2099.
- Allred, A. L. *J. Inorg. Nucl. Chem.* **1961**, *17*, 215.
- Addison, M. C.; Donovan, R. J.; Garraway, J. *Discuss. Faraday Soc.* **1980**, *67*, 286.
- Using $53 \pm 3 \text{ kcal/mol}$ for the bond dissociation energy of IO as reported by Radlein, D. St. A. G.; Whitehead, J. C.; Grice, R. *Nature* **1975**, *253*, 37.
- Weast, R. C. *Handbook of Physics and Chemistry*, 63rd ed.; CRC Press, 1982–83.